Journal of the Serbian Chemical Society
JSCS@tmf.bg.ac.rs • www.shd.org.rs/JSCS

J. Serb. Chem. Soc. 91 (0) 1–18 (2026)
JSCS–13744

Original scientific paper
Published 1 May 2026

In silico evaluation of phycobilins as multi-target anti-tubercular scaffolds: Molecular docking, dynamic stability, ADMET and mycobacterial sensitivity analysis

AMELA K. LEPOJEVIĆ[1], MIROSLAV M. JEVTIĆ[1], MARIO V. ZLATOVIĆ[2] and SRĐAN Đ. STOJANOVIĆ[3]*

[1]*Special Hospital for Pulmonary Diseases and Tuberculosis "Ozren", Sokobanja, Serbia,* [2]*University of Belgrade, Faculty of Chemistry, Department of Organic Chemistry, Belgrade, Serbia and* [3]*University of Belgrade, Institute of Chemistry, Technology and Metallurgy – National Institute of the Republic of Serbia, Department of Chemistry, Belgrade, Serbia*

(Received 24 January, revised 2 February, accepted 5 February 2026)

Abstract: Tuberculosis remains a major global health burden, highlighting the urgent need for novel therapeutic scaffolds with imbproved efficacy and multi--target activity. In this study, an integrated *in silico* strategy was used to investigate the anti-tubercular potential of four naturally occurring phycobilins – phycocyanobilin, phycoerythrobilin, phycourobilin and phycoviolobilin – against a panel of essential *Mycobacterium tuberculosis* protein targets involved in cell wall biosynthesis, nucleic acid metabolism, energy production and ribosomal function. Molecular docking analyses revealed consistently strong binding affinities of phycobilins toward multiple targets, often exceeding those of isoniazid and approaching the binding performance of rifampicin, indicating pronounced multi-target interaction capability. Noncovalent interaction analysis showed stable and diverse interaction networks dominated by hydrogen bonding and hydrophobic contacts. Normal mode analysis confirmed that phycobilin binding preserves intrinsic protein dynamics while inducing ligand-mediated stabilization of the protein–ligand complexes, particularly for the phycoviolobilin–InhA system. Pharmacokinetic and toxicity predictions suggested moderate distribution properties and generally favorable safety profiles, although potential mutagenicity and skin sensitization signals were identified. Additionally, mycoCSM--based predictions indicated micromolar-range anti-mycobacterial activity with limited penetration into caseous lesions. Collectively, these results support phycobilins as promising natural scaffolds for anti-tubercular drug discovery, warranting further optimization and experimental validation.

Keywords: phycobilins; tuberculosis; inhibitors; proteins; *in silico* studies.

* Corresponding author. E-mail: srdjan.stojanovic@ihtm.bg.ac.rs
https://doi.org/10.2298/JSC260124006L

INTRODUCTION

Tuberculosis (TB), caused by *Mycobacterium tuberculosis*, remains a leading cause of mortality from a single infectious agent worldwide, despite established chemotherapeutic regimens. The global rise of multidrug-resistant (MDR) and extensively drug-resistant (XDR) TB strains, along with prolonged treatment durations and dose-limiting toxicities, continues to undermine therapeutic success and highlights the urgent need for novel anti-tubercular agents with improved efficacy and resistance-mitigating properties.[1] These challenges have driven a paradigm shift in TB drug discovery toward strategies that extend beyond single-target inhibition.[2]

The mycobacterial cell is defined by a highly complex and resilient structure, including a lipid-rich cell wall, specialized metabolic pathways, and tightly regulated transcriptional and translational machinery. Key enzymes involved in fatty acid synthesis (such as InhA and KasA), arabinan and peptidoglycan biosynthesis, nucleic acid processing, ribosomal stability and energy production have been validated as drug targets in TB chemotherapy.[3,4] Drugs that interact with those multiple targets may produce synergistic inhibitory effects, reduce bacterial adaptability and enhance sterilizing activity. As a result, multi-target drug discovery has received considerable attention as a rational framework for next-generation TB therapeutics.[5]

Natural products remain a valuable source of structurally diverse and biologically validated scaffolds for antimicrobial drug discovery. Among these, phycobilins are linear tetrapyrrolic pigments derived from cyanobacteria and algae, primarily known for their role in photosynthetic light harvesting and for various reported pharmacological activities, including antioxidant, anti-inflammatory and cytoprotective effects.[6] Their extended conjugated systems, conformational flexibility and extensive hydrogen-bonding capacity suggest an inherent potential to engage diverse protein targets. However, the anti-mycobacterial and molecular interaction profiles of phycobilins remain largely unexplored.

Advances in computational chemistry and structural bioinformatics have enabled the systematic evaluation of multi-target ligand behavior in the early stages of drug discovery. Blind molecular docking allows rapid identification of binding sites and interaction modes across diverse protein targets, while normal mode analysis (NMA) provides critical insight into ligand-induced conformational dynamics and complex stability beyond static affinity metrics.[7–9] In parallel, *in silico* pharmacokinetic, toxicity and pathogen-specific activity prediction platforms facilitate early identification of drug-likeness, safety liabilities and therapeutic relevance, streamlining lead prioritization.[10,11]

In this study, we used an integrated *in silico* workflow to evaluate the anti-tubercular potential of four naturally occurring phycobilins – phycocyanobilin, phycoerythrobilin, phycourobilin and phycoviolobilin – against a diverse panel of

essential *M. tuberculosis* protein targets representing multiple biological processses. By combining molecular docking, noncovalent interaction profiling, normal mode analysis, ADMET prediction and mycobacterial sensitivity modeling, this work assesses the feasibility of phycobilins as multi-target, lead-like scaffolds for rational anti-tubercular drug development.

EXPERIMENTAL

Molecular docking

Chemical structures of the ligands (phycocyanobilin, phycoerythrobilin, phycourobilin, phycoviolobilin, isoniazid and rifampicin) were retrieved in SDF format from the PubChem compound database (http://www.pubchem.ncbi.nlm.nih.gov/search)[12] for subsequent molecular docking and binding affinity analysis. The three-dimensional (3D) structures of the proteins (Table I) were obtained in PDB format from the RCSB Protein Data Bank (https://www.rcsb.org).[13] Docking studies were performed using the CB-Dock2 server (https://cadd.labshare.cn/cb--dock2/),[14] an advanced protein–ligand blind docking server with improved binding site identification and binding pose prediction. The submitted ligand was processed by adding hydrogens and partial charges and an initial 3D conformation was generated using RDKit (RDKit: Open--source cheminformatics, https://www.rdkit.org). CB-Dock2 checks the submitted protein, adds missing side-chain and hydrogen atoms, notifies users of missing residues and removes co--crystallized waters and other heteroatoms. CB-Dock2 performs protein–ligand blind docking by integrating cavity identification, docking and homologous template fitting. It improves blind docking by identifying the protein's binding cavities and generating the predicted dimensions and centers using the latest version of AutoDock Vina (v. 1.2.0).[15] Using these techniques, CB--Dock2 provides more accurate predictions of protein–ligand interactions. Interaction profiles and visualizations were generated for the best-docked complexes. The docked protein–ligand interactions were visualized using Biovia Discovery Studio Visualizer 2025.[16]

Noncovalent interaction analysis

The docked protein and ligand interactions were analyzed and visualized using Biovia Discovery Studio Visualizer 2025 with default-specific criteria and geometrical feature settings.[16]

Normal mode analysis (NMA)

Docked protein–phycobilin complexes were analyzed by normal mode analysis (NMA) using the iMODS server (https://imods.iqf.csic.es).[8] The iMODS platform was used to characterize the structural dynamics and stability of docked complexes by analyzing deformability, B--factors, eigenvalues, variance, covariance maps and elastic network properties. From a single structure, the server calculates the lowest-frequency normal modes using internal coordinates. This dual approach enabled comprehensive assessment of ligand-induced conformational changes and dynamic stability within the protein–phycobiln systems. The computational efficiency of this approach has enabled the evaluation of large-scale motions and dynamic transitions of proteins without excessive computational resources.[8,17] The coarse-grained CA atomic model and the elastic network model were used to balance computational efficiency and accuracy in predicting global motions. The normal mode value indicates motion stiffness, with lower eigenvalues representing simple bending motions in relation to the energy required for these deformations.

Pharmacokinetic and toxicity profiles

ADMET properties refer to drug absorption, distribution, metabolism, excretion and toxicity. They are useful for predicting pharmacological and toxicological characteristics in preclinical stages. We used the freely accessible Deep-PK online tool (https://biosig.lab.uq.edu.au/deeppk/) to evaluate the pharmacokinetics of the phycobilins.[18] The SMILES format of the phycobilins was retrieved from the PubChem database and used as input for the Deep-PK server.

Prediction of anti-tuberculosis sensitivity

In this study, we used the online server mycoCSM (https://biosig.lab.uq.edu.au/myco_csm) to predict the anti-tubercular activity of the phycobilins.[11] The SMILES format of the phycobilins was uploaded as an input form, and the analysis report was downloaded in CSV format. The anti-mycobacterial activity, caseum fraction unbound (FU) and maximum recommended tolerated doses (MRTD) for the phycobilins were determined.

RESULTS AND DISCUSSION

Proteins are essential for maintaining membrane integrity and supporting metabolic functions, making them promising targets for drug development. We used a standard *in silico* approach to investigate the multi-target specificity of phycobilins against protein targets involved in processes ranging from membrane synthesis to nucleic acid metabolism, which are also targeted by antibiotics currently recommended for tuberculosis treatment.[3] Phycobilins were selected for their reported pharmacological activities[6] and serve as representative candidates in this study, which focuses on their therapeutic potential against *Mycobacterium*

TABLE I. The proteins targeted in this study and their corresponding PDB IDs

Target	Function	PDB ID
Enoyl-[acyl-carrier-protein] reductase (NADH)	Build long-chain fatty acids, that form the tough mycobacterial cell wall.	2NSD
KasA	Essential enzyme in the bacterium's unique cell wall synthesis (FAS-II system).	2WGD
Pantothenate synthetase (Mtb PanC)	Vital enzyme in the tuberculosis bacterium's essential pathway for making Coenzyme A.	3COW
Arabinosyl transferase	Responsible enzyme for adding arabinose sugars to build LAM, a vital component of the bacterial cell wall.	3PTY
DNA Gyrase	Introduces negative supercoils into DNA.	4G3N
Ribosomal protein S1	Important protein involved in the functioning of the bacterial ribosome.	4NNI
MurB	Crucial enzyme for building the bacterial cell wall's peptidoglycan layer.	5JZX
2′-*O*-methyltransferase TlyA	Regulate ribosome stability.	5KYG
Protein kinase B	Crucial serine/threonine protein kinase, essential for bacterial growth, cell wall maintenance, division and switching between active replication and dormant states.	5U94
ATP synthase epsilon chain	Vital enzyme for the pathogen's energy production.	5YIO
DNA-directed RNA polymerase	Crucial enzyme for targeting promoters and initiating gene expression.	5ZX3

tuberculosis. In the initial stage of our research, we conducted a molecular docking study of the ligands (phycobilins) to determine their intermolecular interactions with amino acid residues at the active sites of the target proteins (Table I). In the second phase, based on the docking results, we subjected the screened compounds to ADME-Tox and drug-likeness analyses, as well as anti-tuberculosis sensitivity prediction.

Molecular docking studies

Predicting interactions between proteins and small molecules is essential for understanding many biological processes and is crucial for elucidating protein functions and advancing drug development.[19] Protein–ligand blind docking is a powerful approach that identifies the binding regions of a protein and simultaneously predicts the binding pose of a molecule.[20,21] To assess potential efficacy, we performed molecular docking of phycobilins with the target proteins (Table II, Scheme 1). For comparison, Table III presents molecular docking analyses of protein targets with the known anti-tubercular drugs isoniazid and rifampicin. For each protein–ligand pair, five poses were generated using the CB--Dock-2 server. We selected the pose with the highest binding energy and the lowest Vina score, indicating the strongest interaction between the ligand and the protein's active site. This pose represents the most stable complex and demonstrates the affinity and efficacy of these compounds as ligands for the target proteins. The docking scores reported by the CB-Dock-2 server represent relative shape complementarity values, not absolute binding free energies. These correlation-based scores are expressed in arbitrary units scaled to kJ mol^{-1}.

TABLE II. Docking server results for phycobilins

PDB ID	Phycocyanobilin		Phycoerythrobilin		Phycourobilin		Phycoviolobilin	
	Vina score kJ mol^{-1}	Cavity volume Å^3	Vina score kJ mol^{-1}	Cavity volume Å^3	Vina score kJ mol^{-1}	Cavity volume Å^3	Vina score kJ mol^{-1}	Cavity volume Å^3
2NSD	–43.9	2016	–43.5	2016	–43.9	3035	–46.0	2016
2WGD	–29.3	228	–30.5	154	–28.0	154	–28.9	228
3COW	–38.9	3510	–40.6	3510	–41.8	3510	–40.6	3096
3PTY	–38.5	272	–36.0	272	–33.9	272	–35.1	103
4G3N	–35.6	3623	–37.2	3623	–35.1	3623	–33.9	3623
4NNI	–33.9	286	–40.2	286	–31.8	286	–34.7	286
5JZX	–38.9	3638	–38.1	5932	–36.8	7382	–40.6	5139
5KYG	–31.0	322	–32.6	322	–32.2	322	–33.5	322
5U94	–38.5	1704	–40.2	1704	–37.7	1704	–33.5	1704
5YIO	–31.0	242	–32.2	242	–30.1	86	–30.5	86
5ZX3	–37.7	3507	–45.2	3964	–44.8	3964	–41.4	3964

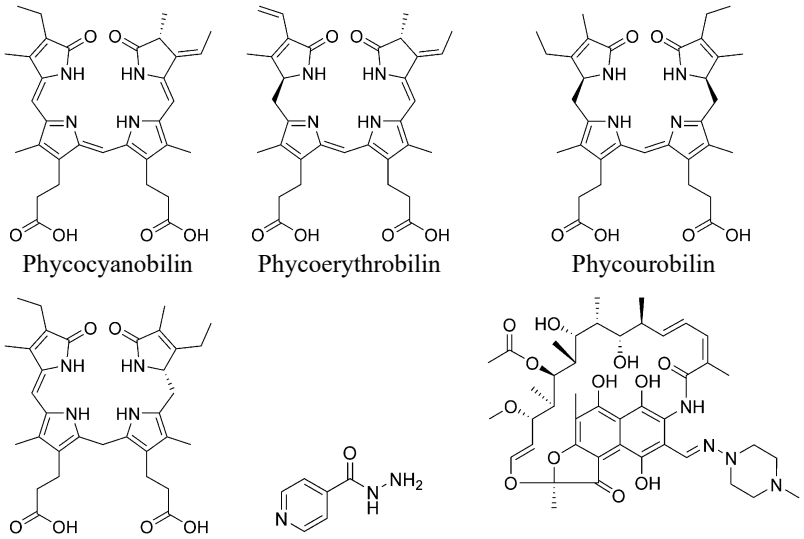

Scheme 1. Structures of phycocyanobilin, phycoerythrobilin, phycourobilin, phycoviolobilin, isoniazid and rifampicin.

TABLE III. Docking server results for antibiotics

PDB ID	Isoniazid		Rifampicin	
	Vina score, kJ mol^{-1}	Cavity volume, Å^3	Vina score, kJ mol^{-1}	Cavity volume, Å^3
2NSD	–25.5	3035	–39.7	3035
2WGD	–25.9	767	–30.5	228
3COW	–24.7	3510	–31.4	3096
3PTY	–24.3	272	–39.3	272
4G3N	–20.1	3623	–36.0	3623
4NNI	–22.2	598	–67.4	598
5JZX	–24.3	7382	–31.0	5932
5KYG	–23.8	183	–32.6	183
5U94	–21.3	362	–33.5	1704
5YIO	–20.5	242	–29.3	242
5ZX3	–25.9	3964	–43.1	13175

It should be emphasized that the Vina scores reported by the CB-Dock2 server represent relative shape complementarity and predicted binding affinity, not absolute experimental binding free energies. These values are useful for ranking and prioritizing potential scaffolds but should be interpreted as theoretical indicators of interaction strength rather than precise thermodynamic measurements.

Molecular docking analyses showed that all four phycobilins had excellent binding affinity for the active sites of the proteins 2NSD, 3COW, 5JZX and 5ZX3 (Vina score < –40 kJ mol^{-1}), indicating their suitability as ligands for these proteins (Table II). In comparison, the docking results showed that the docking scores

of the other target proteins ranged from –28 to –40 kJ mol^{-1}, indicating significant binding affinity. These results suggest that all phycobilins have a stronger predicted binding affinity than the reference antibiotic isoniazid (Table III). In contrast, rifampicin showed docking scores similar to those of the phycobilins and exhibited high affinity for the target proteins. The present study also predicted that the suggested natural compounds may be multi-target specific. The ability to target multiple cellular mechanisms, such as cell wall biosynthesis, nucleic acid synthesis and metabolic integrity of the pathogen, could enhance the potential of these compounds as potent multi-targeted anti-tubercular agents.[4]

Based on molecular docking results showing favorable binding affinities, phycobilins with the lowest Vina scores were selected for further analysis of their interaction profiles with all target proteins, focusing on noncovalent interactions (Table IV).

TABLE IV. Interaction profiles between target proteins and the tested phycobilins

PDB ID	Phycocyanobilin				Phycoerythrobilin				Phycourobilin				Phycoviolobilin			
	N_{HB}[a]	N_{ES}[b]	N_{HP}[c]	N_{O}[d]	N_{HB}	N_{ES}	N_{HP}	N_{O}	N_{HB}	N_{ES}	N_{HP}	N_{O}	N_{HB}	N_{ES}	N_{HP}	N_{O}
2NSD	3	–	13	–	6	–	6	–	5	–	6	–	5	–	5	–
2WGD	5	–	2	–	6	1	–	–	7	–	1	–	5	1	4	–
3COW	4	2	5	–	8	1	3	–	7	1	3	–	9	–	10	–
3PTY	6	1	3	–	7	–	4	–	4	–	4	–	7	1	4	–
4G3N	6	1	2	–	5	1	3	–	6	–	1	–	10	–	5	–
4NNI	9	–	1	–	9	–	1	–	4	1	3	–	5	2	7	–
5JZX	5	–	6	–	6	–	8	–	9	–	7	–	8	–	10	–
5KYG	11	–	1	–	6	–	–	–	6	2	–	–	8	–	5	–
5U94	4	1	5	1	6	–	4	1	5	–	3	–	6	1	4	–
5YIO	7	1	5	–	3	1	4	–	5	–	2	–	6	–	5	–
5ZX3	2	–	5	–	5	–	14	–	7	1	6	–	8	–	7	–

[a]Number of hydrogen bonds; [b]number of electrostatic interactions; [c]number of hydrophobic interactions; [d]number of other interactions

Interaction prediction using Discovery Studio Visualizer software revealed that numerous interactions occur between proteins and ligand molecules. Analysis of the interaction profile showed that, in addition to hydrogen bonds and hydrophobic interactions – the most common types of protein–ligand interactions – phycobilins also form electrostatic interactions with target proteins. Electrostatic interactions are not frequent among protein–ligand interfaces (Table IV). Many interfaces did not form electrostatic interactions, and the maximum number of electrostatic interactions in a complex was two (phycocyanobilin–3COW). For other interactions, there are two π–sulfur interactions in phycobilin complexes with the protein 5U94. Overall, the target protein's ability to support strong, multimodal interactions with phycobilins underscores its value as a central target for rational, structure-based anti-tubercular inhibitor design.

Fig. 1 clearly shows the types of noncovalent interactions and the interacting residues of the complex with the highest binding affinity (phycoviolobilin–2NSD; Vina score, –46.0 kJ mol^{-1}). Hydrogen bonding involves several residues, including Ile21, Ala22, Ser94 and Phe97, indicating a strong hydrogen bond network that enhances the stability of the complex. Ser94 acts as both a donor and an acceptor, simultaneously forming hydrogen bonds with phycoviolobilin. These arrangements may increase stability and play an important role in understanding the three-dimensional structure of protein–ligand complexes. Hydrogen bonding is essential for the specificity and strength of ligand binding, which is important in drug design.[22] A hydrophobic interactions is noted with Phe41, Ile95, Phe149 and Tyr158 (π–sigma and π–alkyl), indicating that these residues contribute to the binding affinity of compounds through nonpolar interactions.

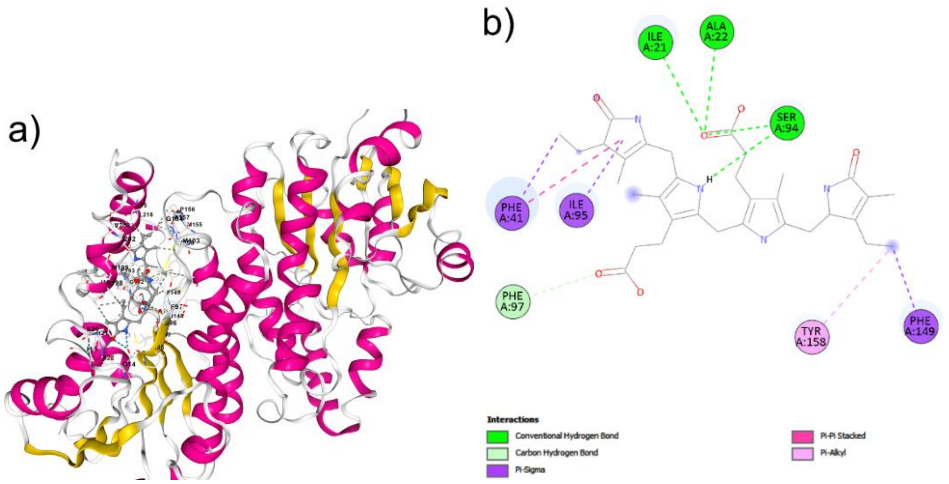

Fig. 1. The best docked complex of phycoviolobilin with 2NSD (Vina score, –46.0 kJ mol^{-1}); a) 3D structure showing the interactions between phycoviolobilin and protein 2NSD; b) 2D diagram of the docked complex.

Normal mode analysis (NMA) of docked complexes

Normal mode analysis (NMA) was performed to assess the intrinsic dynamics and stability of the top-ranked docked protein–phycobilin complexes using a Cα--based elastic network model implemented on the iMODS server. This approach enables characterization of collective motions, flexible distribution, and energetic features that govern the stability of protein–ligand assemblies. The NMA results for the best-docked complex of enoyl-acyl carrier protein reductase InhA (2NSD) with phycoviolobilin are shown in Fig. 2.

The deformability profile (Fig. 2b) shows several pronounced peaks, indicating flexible regions that may act as hinges or adaptive segments around the ligand-

-binding environment. These flexible regions are possibly essential for accommodating phycoviolobilin and allowing subtle conformational rearrangements upon binding. In contrast, the relatively low deformability observed in other regions suggests that the ligand is embedded in a mechanically stable framework, which may enhance binding specificity and reduce structural fluctuations. Such a balance between local flexibility and global rigidity is a hallmark of efficient ligand-binding proteins and has been widely described in elastic network studies of protein–ligand complexes.[23]

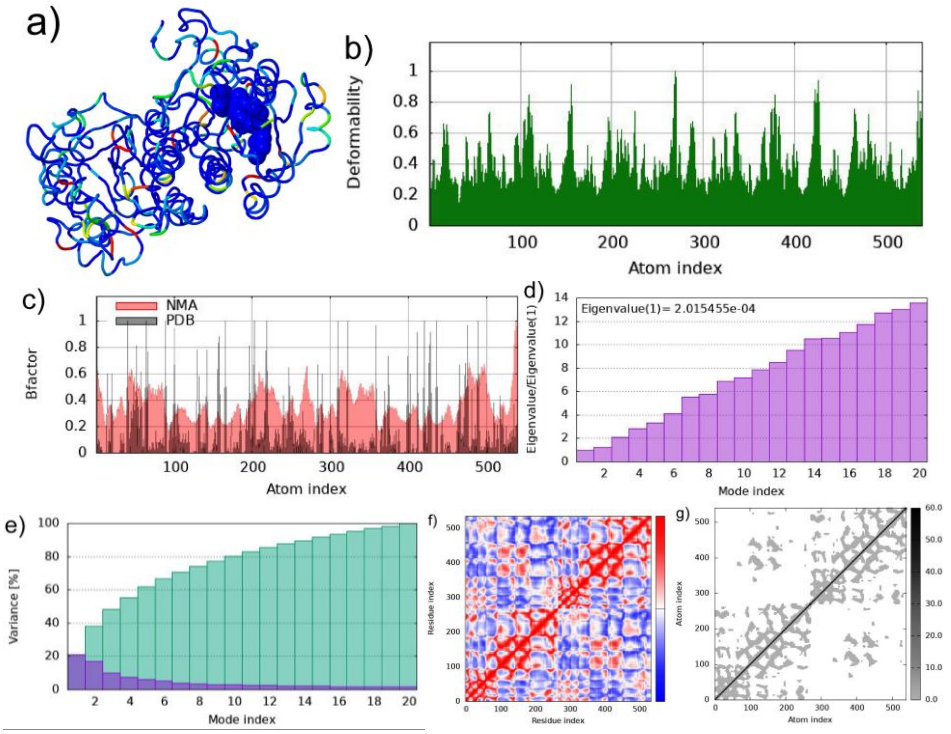

Fig. 2. Normal mode analysis (NMA) of enoyl-acyl carrier protein reductase InhA (2NSD) with the phycoviolobilin structure and its dynamic behavior: a) ligand bound in the binding pocket of the 2NSD protein. Blue: stable regions with low fluctuations; green and yellow: regions with moderate flexibility; orange and red: regions with high mobility; b) deformability plot showing the flexibility of each residue, with peaks indicating regions of high deformability; c) comparison of the normalized B-factors obtained from NMA (red) and from the crystal structure (black), indicating the reliability of the predicted atomic fluctuations; d) eigenvalue associated with each normal mode, reflecting the stiffness of the motion; lower eigenvalues indicate greater deformability; e) the variance associated with normal modes (purple – individual; green – cumulative variances); f) cross-correlation matrix of residue fluctuations, where red denotes correlated motions and blue denotes anti-correlated motions; g) elastic network model showing pairwise atomic connections; darker regions represent stronger interactions.

The comparison of NMA-derived B-factors with experimental B-factors from the crystal structure (Fig. 2c) shows a generally consistent trend throughout the protein sequence. Regions predicted to be flexible or rigid by the NMA model correspond well with experimentally observed atomic fluctuations. The overall consistency supports the conclusion that ligand binding modulates, rather than suppresses, intrinsic protein dynamics.

The eigenvalue spectrum (Fig. 2d) shows a very low eigenvalue for the first normal mode, corresponding to a soft, energetically accessible collective motion. Low-frequency modes are typically associated with global, functionally relevant motions rather than local unfolding events. This indicates that the 2NSD protein maintains its mechanical integrity after ligand binding, and suggests that the ligand is dynamically compatible with the protein's native fold, not destabilizing it.[8]

The variance distribution (Fig. 2e) shows that a small subset of low-frequency modes accounts for most of the protein's motion. Here, the cumulative variance (green bars) quickly saturates within the first 20 modes. This pattern confirms that the dynamics of 2NSD are governed by coordinated global transitions rather than fragmented or random local fluctuations. That behavior characterizes mechanically stable protein–ligand complexes.[24]

The covariance map (Fig. 2f) shows the prevalence of positively correlated motions (red regions) among residue pairs. These large locks of correlation zones along the diagonal indicate coherent domain movements and efficient intramolecular communication. The lack of extensive anti-correlated motions (blue regions) suggests that the bonded ligand does not introduce dynamic strain or conflicting motions between different protein segments, thereby preserving functional coordination. Similar correlation patterns have been associated with stable ligand-bound states in previous NMA studies.[25,26]

The underlying elastic network model shows a dense, well-integrated network of harmonic springs. The high frequency of firmer connections (darker gray dots) throughout the atom-index matrix indicates strong mechanical coupling. The ligand-binding site is nested within this stable, elastic framework and ligand binding appears to strengthen the mechanical integrity of 2NSD rather than disrupt it.

Overall, the NMA results indicate that phycoviolobilin binding stabilizes the global architecture of 2NSD while preserving essential flexibility and long-range correlated motions. The ligand appears to act as a dynamic modulator, reinforcing cooperative motions and maintaining access to low-energy conformational states. These properties are likely crucial for the biological function of the complex, particularly in processes requiring efficient energy transfer or signal propagation.

NMA analysis of other top-docked complexes with phycobilins shows similar results. The atomic conformation pattern was nearly identical for all complexes and remained stable after docking with the phycobilin molecules. These results are provided in the Supplementary material to this paper.

While NMA correctly identifies collective motions and global stability of the docked complexes, it is important to acknowledge its limitations as a first-order harmonic approximation around a single static structure. This analysis does not account for explicit solvent effects, thermal fluctuations, or long-term time-dependent conformational sampling typically captured by molecular dynamics (MD) simulations. Therefore, the NMA results presented here serve as an exploratory validation of complex stability, and further MD studies are warranted.

Pharmacokinetic and toxicity profiles

ADMET plays a crucial role in preclinical testing of drug candidates by enabling assessment of pharmacokinetic and toxicity profiles and facilitating the identification of lead compounds.[27] Therefore, an *in silico* pharmacological and toxicological study was conducted on the phycobilins using the Deep-PK online tool (Table V).

TABLE V. ADMET analysis of the phycobilins obtained with Deep-PK tool; NB – non-bioavailable; NP – non-penetrable; NI – non-inhibitor; I – inhibitor; NS – non-substrate

Absorption category	Phycocyanobilin	Phycoerythrobilin	Phycourobilin	Phycoviolobilin
Caco-2 permeability	–5.66	–5.86	–5.85	–5.72
Human oral bioavailability 20 %	NB	NB	NB	NB
Human intestinal absorption	Absorbed	Absorbed	Absorbed	Absorbed
Skin permeability	Low	Normal	Normal	Low
Distribution category				
Blood–brain barrier	NP	NP	NP	NP
Plasma protein binding	26.13	53.05	52.96	20.64
Fraction unbound (human)	1.39	1.42	1.20	1.41
Steady-state volume of distribution	0.56	0.51	0.50	0.61
Metabolism category				
CYP 1A2 Inhibitor	NI	NI	Inhibitor	NI
CYP 2C19 Inhibitor	NI	NI	NI	NI
CYP 2C9 Inhibitor	NI	NI	NI	NI
CYP 2D6 Inhibitor	NI	NI	NI	NI
CYP 3A4 Inhibitor	NI	NI	NI	NI
CYP 1A2 Substrate	NS	NS	NS	NS
CYP 2C19 Substrate	NS	NS	NS	NS
CYP 2C9, CYP 2D6, CYP 3A4 Substrate	NS	NS	NS	NS
Excretion category				
Clearance	3.86	2.72	3.97	3.41

TABLE V. Continued

Absorption category	Phycocyanobilin	Phycoerythrobilin	Phycourobilin	Phycoviolobilin
Excretion category				
Organic cation transporter 2	NI	NI	NI	NI
Half-life of drug, h	< 3	< 3	< 3	< 3
Toxicity category				
AMES mutagenesis	Toxic	Toxic	Toxic	Toxic
Avian	Safe	Safe	Safe	Safe
Bee	Safe	Safe	Safe	Safe
Biodegradation	Safe	Safe	Safe	Safe
Liver injury II	Safe	Safe	Safe	Safe
Eye corrosion	Safe	Safe	Safe	Safe
Eye irritation	Safe	Safe	Safe	Safe
Maximum tolerated dose	0.07	0.03	0.10	–0.01
HERG blocker	Safe	Safe	Safe	Safe
Skin sensitization	Toxic	Toxic	Toxic	Toxic

Caco-2 cells are commonly used as an *in vitro* model to predict human oral drug absorption.[18] The prediction indicated low Caco-2 permeability for all phycobilins. Additionally, it was estimated that all phycobilins would be orally non-bioavailable in humans but are predicted to be absorbed in the human intestine. Regarding skin permeability, phycocyanobilin and phycoviolobilin were predicted to have low skin permeability, while phycoerythrobilin and phycourobilin were predicted to have normal skin permeability. It is estimated that all phycobilins lack the ability to cross the blood-brain barrier efficiently and are predicted to have an appropriate plasma protein binding value. This is an important therapeutic index related to the amount of free drug in the body. A moderate steady-state volume of distribution was predicted for all phycobilins, indicating a balanced distribution between plasma and tissue. All phycobilins are estimated to be non-inhibitors of cytochrome P450 isoforms, while phycourobilin is predicted to inhibit CYP1A2, an important detoxification enzyme primarily located in the liver. The predominance of non-inhibitor (NI) annotations in the metabolism category suggests that the phycobilins studied are unlikely to inhibit major CYP isoforms, reducing the risk of pharmacokinetic drug–drug interactions.[28] This is particularly important in tuberculosis treatment, where the concurrent use of multiple drugs is common.[4,29]

In terms of excretion, all phycobilins showed a similar clearance rate. Clearance is the rate at which a compound is eliminated through the kidneys and provides an estimate of how long the drug remains in systemic circulation. A higher clearance value indicates that the compound is eliminated from the body more rapidly. The elimination half-life of all phycobilins was short, less than 3 h, sug-

gesting that multiple daily doses may be necessary for therapeutic efficacy. Toxicity prediction showed a generally favorable profile across multiple endpoints, including hERG blockage, liver injury and ocular irritation, with all four bilins predicted to be safe in these areas. However, all compounds were predicted to be AMES--positive (toxic), indicating potential mutagenicity liability and were consistently flagged as toxic for skin sensitization, suggesting possible allergenic potential.

The identification of potential mutagenicity (AMES-positive) and skin sensitization for all four phycobilins is a common challenge in early-stage natural product discovery. These liabilities are frequently observed in natural scaffolds with extended conjugated systems and are typically addressed through systematic lead optimization to separate therapeutic activity from toxicophore signals. Compared to typical early-stage natural product leads, phycobilins have a manageable safety profile that warrants further experimental clarification rather than immediate exclusion.

Given the predicted AMES-positive results, further verification using additional *in silico* toxicity models and experimental *in vitro* AMES assays is required.[30] Structural optimization strategies could be considered to reduce the predicted mutagenic liability during lead optimization. Among the series, the maximum tolerated dose parameter suggested relatively higher tolerance for phycourobilin and lower tolerance for phycoviolobilin, although these differences do not outweigh the consistent AMES and sensitization alerts, which represent critical safety liabilities in early-stage drug development.[31]

Prediction of anti-tuberculosis sensitivity

The anti-tuberculosis potential of phycobilins was evaluated using the mycoCSM web server and compared with the reference antibiotics isoniazid and rifampicin, based on predicted minimum inhibitory concentration (*MIC*), caseum penetration (Caseum FU) and maximum recommended tolerated dose (*MRTD*) (Table VI). The mycoCSM platform uses graph-based signatures to model compound–pathogen interactions and pharmacological properties relevant to tuberculosis drug discovery.[11]

TABLE VI. Anti-tuberculosis sensitivity of phycobilins and antibiotics predicted by mycoCSM; *MIC* – minimum inhibitory concentration; MRTD – maximum recommended tolerated dose

Drug	log (*MIC* / μmol)	Caseum FU, %	log (*MRTD* / mg kg^{-1} day^{-1})
Phycobilins			
Phycocyanobilin	–4.812	3.0	0.726
Phycoerythrobilin	–4.777	5.577	0.656
Phycourobilin	–4.724	3.912	0.524
Phycoviolobilin	–4.991	2.604	0.711
Antibiotics			
Isoniazid	–4.942	67.2	1.166
Rifampicin	–5.809	8.08	0.116

Phycobilins have high molecular weights and extensive hydrogen-bonding capacities, which significantly affect their TB drug-likeness. Although these properties may restrict passive diffusion, they are similar to those of larger macrocyclic anti-tubercular drugs such as rifampicin. The predicted limited penetration into caseous lesions is likely due to these physicochemical parameters (large polar surface area and multiple hydrogen-bond donors), suggesting that future structural modifications should aim to increase lipophilicity and reduce polar surface area to improve intracellular penetration and efficacy in TB-infected tissues.

All four phycobilins showed favorable predicted log (*MIC* / μmol) values, with phycoviolobilin (−4.991) having the lowest *MIC* among the tested bilins, followed by phycocyanobilin (−4.812), phycoerythrobilin (−4.777) and phycourobilin (−4.724). The predicted log *MIC* of phycoviolobilin was comparable to isoniazid (−4.942), though still higher than rifampicin (−5.809), which remains the most potent compound in this comparison. These results suggest that phycobilins, particularly phycoviolobilin, may have moderate to promising anti-mycobacterial activity, supporting their potential as nonclassical anti-tubercular scaffolds, consistent with previous computational TB screening studies.

Caseum FU, a critical parameter for assessing drug accessibility to necrotic TB lesions, was substantially lower for phycobilins (2.6–5.6 %) than for isoniazid (67.2 %) and rifampicin (8.08 %). Limited caseum penetration has been associated with reduced sterilizing activity against *M. tuberculosis* persisting in necrotic granulomas.[32] Among the phycobilins, phycoerythrobilin had the highest caseum FU (5.577 %), indicating relatively better lesion penetration within this group, although still lower than that of the first-line drugs. Given the limited penetration into caseous lesions, future research may benefit from developing nano-based formulations or structural optimization strategies to improve drug distribution within tuberculosis lesions.[33,34]

The predicted log (*MRTD* / mg kg^{-1} day^{-1}) values for phycobilins ranged from 0.524 to 0.726, which are lower than that of isoniazid (1.166) but notably higher than that of rifampicin (0.116). This intermediate *MRTD* profile suggests a moderate tolerability margin, consistent with natural product-derived scaffolds and supports the feasibility of further optimization.[35] Slightly higher *MRTD* values for phycocyanobilin and phycoviolobilin may indicate a comparatively more favorable safety window within this series, consistent with the established relationship between tolerable dose limits and therapeutic safety margins in early-stage drug development.[31,36]

CONCLUSIONS

This study presents a comprehensive and internally consistent computational framework that identifies phycobilins as a promising and underexplored class of natural product scaffolds for anti-tubercular drug discovery. Through systematic

multi-target docking against a broad panel of essential *M. tuberculosis* proteins, phycobilins showed strong and reproducible binding affinities that not only exceeded those of isoniazid across several targets but also approached the interaction strength of rifampicin. This convergence of high-affinity binding across mechanistically diverse enzymes strongly supports a true polypharmacological mode of action, a feature increasingly recognized as critical for overcoming resistance in tuberculosis therapy.

Beyond static affinity predictions, dynamic analyses provided decisive mechanistic insight. Normal mode analysis revealed that phycobilin binding induces ligand-driven stabilization of protein architectures while preserving low-frequency collective motions associated with enzymatic function. This dynamic compatibility, exemplified by the phycoviolobilin–InhA complex, underscores the ability of these ligands to integrate into functional protein networks without imposing destabilizing conformational strain, an essential attribute for sustained inhibitory activity.

Although pharmacokinetic and toxicity predictions indicated limitations in oral bioavailability, lesion penetration, and potential genotoxic and sensitization liabilities, these findings should be interpreted in the context of early-stage lead identification. Importantly, none of these liabilities undermine the central observation that phycobilins have a highly favorable binding and dynamic interaction profile. Instead, they define a clear and rational optimization path focused on improving exposure and safety while preserving intrinsic multi-target potency.

Collectively, the strength and coherence of the computational evidence presented here elevate phycobilins from passive bioactive pigments to strategically valuable lead-like molecules. Their demonstrated capacity for multi-target engagement, dynamic stabilization and competitive inhibitory potential justifies their prioritization for structure-guided optimization and experimental validation, with the long-term prospect of contributing to the development of next-generation anti--tubercular therapeutics. Given the reported limitations in penetration into caseous lesions, future research should explore nano-formulation approaches or rational chemical modifications to improve drug delivery and accumulation at the infection site.

SUPPLEMENTARY MATERIAL

Additional data and information are available electronically at the pages of journal website: https://www.shd-pub.org.rs/index.php/JSCS/article/view/13744, or from the corresponding author on request.

Acknowledgement. This research has been financially supported by the Ministry of Science, Technological Development and Innovation of Republic of Serbia (Contract No: 451-03--136/2025-03/200026 and 451-03-136/2025-03/200168).

ИЗВОД

IN SILICO ЕВАЛУАЦИЈА ФИКОБИЛИНА КАО ВИШЕЦИЉНИХ АНТИТУБЕРКУЛАРНИХ СКЕЛА: МОЛЕКУЛАРНИ ДОКИНГ, ДИНАМИЧКА СТАБИЛНОСТ, ADMET И АНАЛИЗА ОСЕТЉИВОСТИ НА МИКОБАКТЕРИЈЕ

АМЕЛА К. ЛЕПОЈЕВИЋ[1], МИРОСЛАВ М. ЈЕВТИЋ[1], МАРИО В. ЗЛАТОВИЋ[2] и СРЂАН Ђ. СТОЈАНОВИЋ[3]

[1]Специјална болница за плућне болести и туберкулозу „Озрен", Сокобања, [2]Универзитет у Београду, Хемијски факултет, катедра за органску хемију, Београд и [3]Универзитет у Београду, Институт за хемију, технологију и металургију, Центар за хемију, Институт од националног значаја за Републику Србију, Београд

Туберкулоза и даље представља велики глобални здравствени терет, што наглашава хитну потребу за новим терапијским третманом са побољшаном ефикасношћу и вишеструким дејством. У овој студији примењена је интегрисана *in silico* стратегија за испитивање антитуберкулозног потенцијала четири природно присутна фикобилина – фикоцијанобилина, фикоеритрибилина, фикоуробилина и фиковиолобилина – против панела есенцијалних протеинских мета *Mycobacterium tuberculosis* укључених у биосинтезу ћелијског зида, метаболизам нуклеинских киселина, производњу енергије и функцију рибозома. Анализе молекулског докинга показале су конзистентно јак афинитет везивања фикобилина према више циљних протеина, често премашујући афинитет везивања изониазида и приближавајући се перформансама везивања рифампицина, што указује на изражену способност интеракције са више циљева. Анализа нековалентних интеракција указала је на стабилне и разноврсне интеракционе мреже којима доминирају водоничне везе и хидрофобни контакти. Анализа нормалних модова потврдила је да везивање фикобилина очувава својствену динамику протеина, уз истовремено индуковану, лигандима посредовану стабилизацију протеинско–лигандних комплекса, нарочито у систему фиковиолобилин–ИнхА. Предикције фармакокинетике и токсичности указале су на умерена дистрибуциона својства и генерално повољне безбедносне профиле, иако су идентификовани потенцијални сигнали мутагености и сензибилизације коже. Додатно, предвиђања заснована на mycoCSM указале су на антимикобактеријску активност у микромоларном опсегу са ограниченим продирањем у казеозне лезије. Заједно посматрано, ови резултати подржавају фикобилине као обећавајуће природне скеле за откривање лекова против туберкулозе, што захтева даљу оптимизацију и експерименталну валидацију.

(Примљено 24. јануара, ревидирано 2. фебруара, прихваћено 5. фебруара 2025)

REFERENCES

1. B. D. Daniel, C. Padmapriyadarsini, S. Giri, P. S. Winarni, *BMJ* **390** (2025) 2024 (https://doi.org/10.1136/bmj-2024-080075)
2. M. Kufa, V. Finger, O. Kovar, O. Soukup, C. Torruellas, J. Roh, J. Korabecny, *Acta Pharm. Sin., B* **15** (2025) 1311 (https://doi.org/10.1016/j.apsb.2025.01.023)
3. R. R. Patel, Vidyasagar, S. K. Singh, M. Singh, *Microb. Pathog.* **203** (2025) 107515 (https://doi.org/10.1016/j.micpath.2025.107515)
4. A. Zumla, P. Nahid, S. T. Cole, *Nat. Rev. Drug Discov.* **12** (2013) 388 (https://doi.org/10.1038/nrd4001)
5. N. Rao, V. D. Jathar, *Pharm. Chem. J.* **59** (2025) 512 (https://doi.org/10.1007/s11094-025-03422-z)
6. C. García-Gómez, D. E. Aguirre-Cavazos, A. Chávez-Montes, J. M. Ballesteros-Torres, A. A. Orozco-Flores, R. Reyna-Martínez, Á. D. Torres-Hernández, G. M. González-Meza,

S. L. Castillo-Hernández, M. A. Gloria-Garza, M. Kačániová, M. Ireneusz-Kluz, J. H. Elizondo-Luevano, *Mar. Drugs* **23** (2025) 201 (https://doi.org/10.3390/md23050201)
7. I. Kolossváry, *JACS Au* **4** (2024) 1303 (https://doi.org/10.1021/jacsau.4c00109)
8. J. R. López -Blanco, J. I. Aliaga, E. S. Quintana-Orti, P. Chacón, *Nucleic Acids Res*. **42** (2014) W271-W276 (https://doi.org/10.1093/nar/gku339)
9. M. S. Roomi, G. Culletta, L. Longo, W. Filgueira de Azevedo, U. Perricone, M. Tutone, *Pharmaceuticals* **18** (2025) 1777 (https://doi.org/10.3390/ph18121777)
10. R. Ancuceanu, B. E. Lascu, D. Drăgănescu, M. Dinu, *Pharmaceutics* **17** (2025) 1002 (https://doi.org/10.3390/pharmaceutics17081002)
11. D. E. V. Pires, D. B. Ascher, *J. Chem. Inf. Model.* **60** (2020) 3450 (https://doi.org/10.1021/acs.jcim.0c00362)
12. S. Kim, J. Chen, T. Cheng, A. Gindulyte, J. He, S. He, Q. Li, B. A. Shoemaker, P. A. Thiessen, B. Yu, L. Zaslavsky, J. Zhang, E. E. Bolton, *Nucleic Acids Res.* **51** (2023) D1373 (https://doi.org/10.1093/nar/gkac956)
13. H. M. Berman, J. Westbrook, Z. Feng, G. Gilliland, T. N. Bhat, H. Weissig, I. N. Shindyalov, P. E. Bourne, *Nucleic Acids Res*. **28** (2000) 235 (https://doi.org/10.1093/nar/28.1.235)
14. Y. Liu, X. Yang, J. Gan, S. Chen, Z. X. Xiao, Y. Cao, *Nucleic Acids Res*. **50** (2022) W159-W164 (https://doi.org/10.1093/nar/gkac394)
15. J. Eberhardt, D. Santos-Martins, A. F. Tillack, S. Forli, *J. Chem. Inf. Model.* **61** (2021) 3891 (https://doi.org/10.1021/acs.jcim.1c00203)
16. D.S. Biovia, *Discovery Studio Visualizer*, San Diego, CA, 2025
17. X. Q. Yao, L. Skjaerven, B. J. Grant, *J. Phys. Chem., B* **120** (2016) 8276 (https://doi.org/10.1021/acs.jpcb.6b01991)
18. Y. Myung, A. G. C. de Sá, D. B. Ascher, *Nucleic Acids Res.* **52** (2024) W469 (https://doi.org/10.1093/nar/gkae254)
19. B. P. Brown, *Proc. Natl. Acad. Sci. USA* **122** (2025) e2508998122 (https://doi.org/10.1073/pnas.2508998122)
20. C. Hetényi, D. van der Spoel, *Prot. Sci*. **11** (2002) 1729 (https://doi.org/10.1110/ps.0202302)
21. S. Y. Ugurlu, *J. Comput. Aided Mol. Des*. **39** (2025) 48 (https://doi.org/10.1007/s10822-025-00629-w)
22. A. S. Mahadevi, G. N. Sastry, *Chem. Rev*. **116** (2016) 2775 (https://doi.org/10.1021/cr500344e)
23. L. W. Yang, E. Eyal, C. Chennubhotla, J. Jee, A. M. Gronenborn, I. Bahar, *Structure* **15** (2007) 741 (https://doi.org/10.1016/j.str.2007.04.014)
24. T. Ichiye, M. Karplus, *Proteins* **11** (1991) 205 (https://doi.org/10.1002/prot.340110305)
25. F. Tama, Y. H. Sanejouand, *Protein Eng.* **14** (2001) 1 (https://doi.org/10.1093/protein/14.1.1)
26. I. Bahar, T. R. Lezon, L. W. Yang, E. Eyal, *Ann. Rev. Biophys.* **39** (2010) 23 (https://doi.org/10.1146/annurev.biophys.093008.131258)
27. H. van de Waterbeemd, E. Gifford, *Nat. Rev. Drug Discov.* **2** (2003) 192 (https://doi.org/10.1038/nrd1032)
28. U. M. Zanger, M. Schwab, *Pharmacol. Ther*. **138** (2013) 103 (https://doi.org/10.1016/j.pharmthera.2012.12.007)
29. World Health Organization, *WHO consolidated guidelines on tuberculosis: Module 4 – Treatment*, World Health Organization, Geneva, 2023 (https://www.who.int/publications/i/item/9789240107243)

30. R. Benigni, C. Bossa, *Chem. Rev.* **111** (2011) 2507 (https://doi.org/10.1021/cr100222q)
31. P. Y. Muller, M. N. Milton, *Regul. Toxicol. Pharmacol.* **63** (2012) 388 (https://doi.org/10.1016/j.yrtph.2012.05.003)
32. B. Prideaux, L. E. Via, M. D. Zimmerman, S. Eum, J. Sarathy, P. O'Brien, C. Chen, F. Kaya, D. M. Weiner, P. Y. Chen, T. Song, M. Lee, T. S. Shim, J. S. Cho, W. Kim, S. N. Cho, K. N. Olivier, C. E. Barry, III, V. Dartois, *Nat. Med.* **21** (2015) 1223 (https://doi.org/10.1038/nm.3937)
33. T. Bourguignon, JA. Godinez-Leon, R. Gref, *Pharmaceutics* **15** (2023) 393 (https://doi.org/10.3390/pharmaceutics15020393)
34. A. Sharma, V. Sharma, S. Sharma, S. Sharma, M. Sharma, I. Sivanesan, *Pharmaceutics* **17** (2025) 1459 (https://doi.org/10.3390/pharmaceutics17111459)
35. V. Dartois, *Nat. Rev. Microbiol.* **12** (2014) 159 (https://doi.org/10.1038/nrmicro3200)
36. R. Zhang, H. Wen, Z. Lin, B. Li, X. Zhou, *Toxics* **13** (2025) 525 (https://doi.org/10.3390/toxics13070525).